Susceptibility Mapping in Rat Deep Brain Structures using UHF MRI

D. A. Rudko[1], L. M. Klassen[1], S. N. de Chickera[2], G. A. Dekaban[2], and R. S. Menon[1]
[1]Centre for Functional and Metabolic Mapping, Robarts Research Institute, London, Ontario, Canada, [2]Biotherapeutics Research Group, Robarts Research Institute, London, Ontario, Canada

Introduction: The magnetic susceptibility of rat brain tissue provides a unique source of contrast between grey matter (GM) and white matter (WM). Moreover, ultra high field (UHF) MRI produces larger susceptibility induced field shifts compared to conventional low field MRI, resulting in increased contrast-to-noise ratio (CNR) in phase images. This increased CNR can be used to obtain an improved estimate of microscopic field (μB_0) maps around such susceptibility inclusions as deoxyhemoglobin containing veins (Fig. 1b blue arrow), myelin (Fig. 1b red arrow) and non-heme iron proteins of the subcortical GM (Fig. 1b yellow arrow). In this study, we measured microscopic field (μB_0) maps at 9.4 T in excised, healthy rat brain, to determine field shifts around susceptibility inclusions. The experimentally measured field shifts were compared to the generalized Lorentzian model (GLmodel) proposed by He and Yablonskiy [2]. Additionally, χ-mapping applying a priori knowledge of the susceptibility boundaries from gradient-echo magnitude images was employed to estimate the χ maps [4]. χ and R_2^* maps were also used to determine estimates of iron concentration in relevant tissue micro-structures.

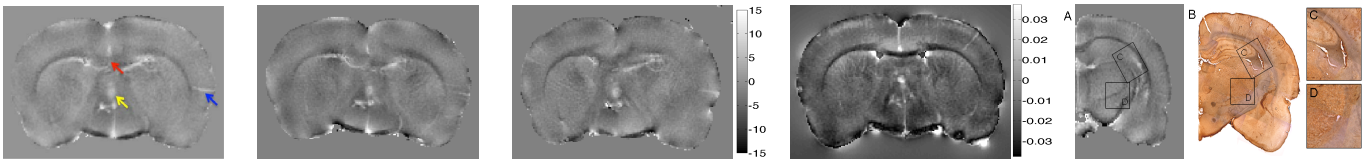

Fig. 1:(a) μB_0 map (Hz), θ = 0° b) μB_0 map (Hz), θ = 30° (c) μB_0 map (Hz), θ = -30° (d) χ map (ppm) (e) A. μB_0 map (Hz) B/C/D iron stain

Methods: Rat brains were excised from male Sprague Dawley rats and fixed in formalin solution to preserve brain tissue, micro-structural features prior to imaging. For imaging, the brains were placed inside a 2.5 cm diameter sphere filled with an MR-invisible Christo-Lube solution to minimize the formation of susceptibility artifacts at the edges of the brain tissue. The spherical sample holder allowed accurate rotation of the rat brain in order to image it at different sampling angles relative to the main B_0 field of the magnet. Imaging was performed using a 3D multi-echo gradient echo sequence. An imaging field of view of 19.2 x 19.2 x 19.2 mm^3, an in-plane resolution of 100 μm and a slice thickness of 600 μm were used. Raw B_0 field maps were derived from phase images that were unwrapped using a second derivative minimization temporal unwrapping [3]. Maps were acquired with the rat brain rotated at angles ranging from – 90° to + 90° about the x-axis of the magnet frame (sampling angles of -30°, 0° and 30° are analyzed below). To remove background fields, a 15th-order 3D polynomial was fitted to the field maps. The fitted maps were then subtracted from the raw B_0 field maps to calculate μB_0. Susceptibility map reconstruction was completed utilizing an L2-quadratic minimization [4]. After imaging, the rat brain was sectioned into 50 μm slices and stained with a DAB-enhanced Perls stain to display regions where endogenous iron and field shifts in the μB_0 maps were co-localized (Fig. 1e – representative slice). The following formulas from the GLmodel were applied for calculating frequency shifts:

	Cerebral Veins	WM (corpus callosum) *	Subcortical GM
μB_0 (Hz), θ = 0°	4.41 ± 1.11	-3.90 ± 0.43	4.58 ± 0.57
GLmodel (Hz),θ = 0°	3.18 ± 0.81	(i) 4.79 ± 0.86 (ii) -2.40 ± 0.43	5.85 ± 1.22
μB_0 (Hz), θ = 30°	5.78 ± 0.85	-2.76 ± 0.85	5.63 ± 0.65
GLmodel (Hz), θ = 30°	5.37 ± 0.81	(i) 2.59 ± 0.47 (ii)-1.50 ± 0.27	5.85 ± 1.22
μB_0 (Hz), θ = -30°	5.31 ± 1.38	- 2.84 ± 0.66	5.21 ± 1.26
GLmodel (Hz), θ = -30°	5.37 ± 0.81	(i) 2.59 ± 0.47 (ii)-1.50 ± 0.27	5.85 ± 1.22
L2 χ (ppm), θ = 0°	0.013 ± 0.005	-0.026 ± 0.002	0.028 ± 0.007
Tissue Iron from $R2^*$ (nmol/g tissue wet weight [1])	0.242 ± 0.011	0.272 ± 0.009	0.317 ± 0.019
Tissue Iron from χ (nmol/g)	0.155 ± 0.006	0.309 ± 0.002	0.334 ± 0.083

Table 1: Measured and theoretical μBo and mapped iron concentrations.
***(i) = Elliptical cylinder approximation to white matter axon bundle.**
(ii) = Circular cylinder approximation to white matter axon bundle in isotropic media.

$$\frac{\Delta f_{GM}}{f_o} = \frac{4}{3}\pi\lambda\chi_{GM} \quad ; \quad (\lambda = 1) \tag{1}$$

$$\frac{\Delta f_{veins}}{f_o} = \frac{4}{3}\pi \mathrm{DBV}\cdot\Delta\chi_0 \mathrm{Hct}\,(1 - Y) + 2\pi\chi_{GM}\sin^2\theta \tag{2}$$

$$\text{(i)}\quad \frac{\Delta f_{WM}}{f_o} = \frac{4}{3}\pi\chi_{WM} - 2\pi\chi_{GM}(\cos^2\alpha_c - \frac{1}{3}) - 4\pi(\chi_{WM} - \chi_{GM})(N_a\cos^2\alpha_a + N_b\cos^2\alpha_b) \tag{3}$$

$$\text{(ii)}\quad \frac{\Delta f_{WM} - \Delta f_e}{f_o} = -2\pi\cdot(\chi_{GM} - \chi_{WM} + \chi_{GM})(\cos^2\alpha_c - \frac{1}{3}) \tag{4}$$

Results and Discussion: Measured μB_0 maps were used to interpret the validity of the GLmodel. Field shifts in WM, cerebral veins and the basal ganglia were compared to the model frequency shifts. The following literature values from [2] were used with the GLmodel: χ_{WM} = 5.57 x 10^{-3} ppm, χ_{GM} = 3.50 x 10^{-3} ppm, DBV = 1.56 %, $\Delta\chi_0$ = 0.27 ppm, Hct = 0.45, and Y = 0 (DBV, $\Delta\chi_0$, Hct and Y were used for GLmodel calculation in cerebral veins). The GLmodel compares most accurately with mean μB_0 field shifts in subcortical GM and in cerebral veins (see Table 1). This may be due to the more complex dependence of MR field shifts in WM to orientation and structure of axons. The enhanced complexity of the WM field shifts was addressed by examining two theoretical models: (i) the elliptical cylinder and (ii) the circular cylinder approximation. The circular cylinder approximation produced negative field shifts characteristic of cholesterol and phospholipid-like inclusions whose volume magnetic susceptibility is approximately -0.004 to -0.035 ppm in human WM [2]. The improved accuracy of the circular cylinder approximation suggests that equation (4) may provide a more accurate estimate of field shift in WM. Both μB_0 and reconstructed χ in the subcortical GM and WM regions were comparable to χ-values of 0.015 ppm produced at WM/GM cortex interfaces in human brain at 7 T [2]. χ (Fig. 1d) and R_2^* (not shown) maps were used to estimate tissue iron independently, using (i) the linear dependence of $R2^*$ on tissue iron concentration with slope 0.05 Hz/T/ppm taken from [1] and (ii) the molar susceptibility Fe^{3+} compounds at 310 K of 177 ppm L/mol [4]. χ-maps were able to independently cross-validate R_2^*-based iron mapping methods. χ-mapping may provide an improved estimate of iron concentration by removing the influence of background fields which contaminate measurements performed using R_2^* maps.

References: 1) Fukunaga et al. PNAS 2009 ; 107 : 3834 – 3839. (2) He et al. PNAS 2009 ; 106 13558 - 13563 (3) Klassen et al. MRM 2004 ; 51: 881 – 887. (4) Rochefort et al. MRM 2010 ; 63 :194-206.

Acknowledgements : The author thanks Joe Gati and Alex Li for their helpful discussions and acknowledges the support of the Natural Science and Engineering Research Council (NSERC) of Canada, the Canada Research Chairs Program (R.S.M.) and the Robarts Research Institute.